The neural representation of body part concepts

Stephen Mazurchuk [iD][1,2], Leonardo Fernandino[1,3], Jia-Qing Tong[1,2], Lisa L. Conant[1], Jeffrey R. Binder[1,2,*]

[1]Department of Neurology, Medical College of Wisconsin, 8701 Watertown Plank Road, Milwaukee, WI 53226, United States
[2]Department of Biophysics, Medical College of Wisconsin, 8701 Watertown Plank Road, Milwaukee, WI 53226, United States
[3]Department of Biomedical Engineering, Medical College of Wisconsin, 8701 Watertown Plank Road, Milwaukee, WI 53226, United States

*Corresponding author: Department of Neurology, Medical College of Wisconsin, 8701 Watertown Plank Road, Milwaukee, WI 53226, United States.
Email: jbinder@mcw.edu

Neuropsychological and neuroimaging studies provide evidence for a degree of category-related organization of conceptual knowledge in the brain. Some of this evidence indicates that body part concepts are distinctly represented from other categories; yet, the neural correlates and mechanisms underlying these dissociations are unclear. We expand on the limited prior data by measuring functional magnetic resonance imaging responses induced by body part words and performing a series of analyses investigating the cortical representation of this semantic category. Across voxel-level contrasts, pattern classification, representational similarity analysis, and vertex-wise encoding analyses, we find converging evidence that the posterior middle temporal gyrus, the supramarginal gyrus, and the ventral premotor cortex in the left hemisphere play important roles in the preferential representation of this category compared to other concrete objects.

Key words: semantics; categories; body representation; functional MRI; representational similarity analysis.

Introduction

The organization of conceptual knowledge in the brain is a topic of intense study in cognitive neuroscience. Modern theories of semantic representation are informed by studies of patients who, following focal brain damage, present with semantic impairments that disproportionally affect 1 semantic category (e.g. animals) relative to other categories. This phenomenon, hereafter called a category-related semantic deficit (CRSD), has led to competing theories about the nature of semantic representation. Although the category of body part concepts has shown both selective impairment (Suzuki et al. 1997) and sparing (Shelton et al. 1998) after focal brain damage, the extant functional magnetic resonance imaging (fMRI) literature on body part representation almost exclusively focuses on the perception of pictorial stimuli (Downing et al. 2001) without a clear distinction between high-level visual perceptual and postperceptual concept representations. The dearth of fMRI studies using linguistic stimuli to investigate the neural substrate of body part concepts limits our ability to discriminate between perceptual and conceptual processes when relating these findings to CRSDs. This is important because this neuropsychological phenomenon, typically detected through performance impairments on semantic tasks, is considered an impairment of conceptual knowledge rather than visual perception. Filling this knowledge gap could help resolve ongoing debates regarding the dissociable components of body-part knowledge (Vignemont 2007; Longo et al. 2010; Vignemont 2010) and the involvement of particular cortical areas in its representation (Schwoebel and Coslett 2005; Kemmerer and Tranel 2008; Boccia et al. 2020).

One proposed model of body representation in the brain—the dyadic taxonomy (Paillard 1999)—distinguishes between *body schema,* a dynamic representation of current body part positions that can be thought of as a low-level sensory representation of the body, and *body image*, a representation that is semantic in nature and includes long-term knowledge about "what" body parts are. Another proposed model is the triadic taxonomy (Schwoebel and Coslett 2005), which splits the body image representation further into the *body structural description*, a fixed topological map of body locations and boundaries, and *body semantics*, which includes knowledge of body part names, functions, and relations with artifacts (Boccia et al. 2020). Kemmerer and Tranel (2008) argue that the body structural description is essentially semantic in nature, and they divide body semantics (body image in the dyadic taxonomy) into 4 components representing knowledge of body part shapes, locations, functions, and "cultural associations", each proposed to have somewhat distinct neural correlates. In the current study, we operationally define body-related semantic knowledge as any information activated by body part words that cannot be attributed to word-form (orthographic and phonological) properties of the stimuli. Such information could include any of the types of knowledge described by Kemmerer and Tranel.

At present, there is debate about whether body part concept knowledge is functionally and anatomically dissociable from other categories of lexical concepts. Although most reviews of data from brain damaged individuals concluded that body part knowledge is typically spared (Goodglass et al. 1966; Capitani et al. 2003; Gainotti 2004), there is clear evidence that selective impairment of this category can occur (Warrington and McCarthy 1987; Sacchett and Humphreys 1992; Suzuki et al. 1997; Schwoebel and Coslett 2005; Laiacona et al. 2006; Kemmerer and Tranel 2008). Although most of these patients had large lesions, the 3 reported by Schwoebel and Coslett (2005) with selective impairment of body–related functional and associative knowledge all had damage confined to the left temporal lobe, with maximal overlap in the posterior middle temporal gyrus (pMTG, part of Brodmann area 37).

Previous fMRI work using body part words as stimuli is limited to 2 studies using voxel-wise mass univariate analysis, both of which had relatively few participants and few stimuli (Le Clec'H et al. 2000; Goldberg et al. 2006). Goldberg et al. (2006) found that a task requiring similarity judgments on items from the "functionally biased" categories of body parts and clothing activated the left pMTG in comparison to items from 2 "visually biased" categories (fruits and birds). Le Clec'H et al. (2000) reported greater activation during a location judgment task on body part names ("Is it above or below the shoulders?") compared to a judgment task on numbers ("Is it less than 12?") in the left intraparietal sulcus (IPS) and several left frontal regions. Our aim is to expand on this work and clarify the neural correlates of body part concept representations, both on their own and relative to other categories of concrete object nouns. We define a region as involved in the semantic representation of a category if the region's activation is modulated by a semantic variable (e.g. category membership or other semantic feature content such as imageability), and that modulation is not otherwise accountable by visual or ortho–phonological properties of the stimuli. To minimize the influence of these and other potential confounds in the stimuli, we examined the preferential representation of body part concepts using explicit models of semantic content. We used 2 different kinds of models: the 65-dimensional model of concept representation as experiential (i.e. embodied) attributes (hereafter, the CREA model; Binder et al. 2016) and a popular distributional semantic model (Word2Vec; Mikolov et al. 2013).

We hypothesized that body part concepts would be preferentially represented in the left pMTG region, based on the lesion analysis of Schwoebel and Coslett (2005), the proximity of this region to lateral occipitotemporal areas specialized for visual perception of body parts (Spiridon et al. 2006; Orlov et al. 2010; Bracci et al. 2015), and on strong fMRI evidence linking the pMTG with representation of object-directed actions, where body parts are effectors (Jastorff et al. 2010; Oosterhof et al. 2010; Lingnau and Downing 2015). Complementary analyses that address different aspects of representation were conducted to identify convergent results across univariate and multivariate analysis strategies.

Our analyses are divided into those that are independent of an explicit model of semantic content (e.g. standard univariate contrasts between categories) and those that depend on a model of semantic content. We first performed a univariate analysis contrasting activation elicited by body part words to activation elicited by each of 3 other concrete noun semantic categories (animals, plants/foods, and manipulable artifacts). These pairwise comparisons were then entered into a conjunction analysis to determine if there are regions where, in the context of a general semantic judgment task, body part words elicit greater activation than words from other categories. Complementing this univariate analysis, multivoxel pattern analysis (MVPA) was performed to identify regions of the cortex where category identity can be decoded from activation patterns across voxels. This analysis assumes that regions of cortex where category identity can be decoded from activation patterns carry semantic information that is relevant to that category. Specifically, we used searchlight MVPA to compare the ability of a pattern classifier to discriminate body parts from other categories relative to the classifier's ability to discriminate other categories from each other.

A final model-free analysis assessed the reliability of the neural representational geometry of body part concepts across participants. Our interest in performing reliability analysis stems from its relation to a fundamental property of lexical semantic representations. At a minimum, these representations encode the relative similarity (or dissimilarity) among items, and this similarity structure must be shared across participants. For example, many semantic models encode the relation that "birds" and "airplanes" are more similar than "birds" and "computers". The "neural similarity" between pairs of words can be computed by comparing the multivoxel activation patterns they evoke, and the global representational geometry of the neural space can be computed as a matrix of all such pairings, referred to as the neural representational dissimilarity matrix (neural RDM; Kriegeskorte et al. 2008). Since neural RDMs quantify relationships between experimental conditions, operationalizing the previous definition of semantics implies a requirement of similarity in neural RDMs across participants to claim that semantic content is represented. This between-participant similarity can be quantified in reliability metrics such as noise ceilings and intraclass correlation coefficients (ICCs). We emphasize, however, that while a shared representational geometry is a prerequisite for many definitions of a semantic space, it is not sufficient to establish the presence of semantic content. For example, visual word stimuli evoke similar neural representational geometries in the primary visual cortex across participants, even though this shared representation is due to similarities in visual form, not in semantics. Performing searchlight RDM reliability analysis allows us to identify all the regions of cortex where any kind of information about the stimulus set is encoded. In areas where the ICC is too low, there is no information that could be explained by a similarity model (semantic, phonological, or otherwise). To investigate regions that preferentially represent body part knowledge, we searched for regions that had greater shared variance across body part words than across items from other categories of words.

The model-based analyses included a cortical surface-based searchlight representational similarity analysis (RSA) and a vertex-wise encoding analysis. To test whether the semantic models capture the representational geometry among body part concepts, we performed searchlight RSA restricted to body part concepts. To assess whether the semantic models predicted any body part selective regions, we calculated RSA correlations for each category and searched for regions that had higher RSA scores for the body part category compared to any of the other categories. These analyses aim to identify regions where activation patterns capture differences between body part concepts more than differences between items within other categories. This is relevant to defining a "category-preferring" region because CRSDs are typically characterized by an inability to discriminate between items *within* a category, rather than by an inability to determine if an item belongs to a particular category.

Lastly, 1 prediction of embodied theories of semantics is that CRSDs arise from spatial constraints imposed by perceptual processing areas relevant to the affected category. We used encoding models to test whether activation differences that appear to be categorical in nature can be explained by feature content that, although shared across categories, is more important for some categories than for others. Specifically, we tested whether any univariate results showing increased activation to body part concepts relative to other categories of concepts are predicted by semantic encoding models trained using concepts outside the body part category.

Materials and methods

Relative to many fMRI studies of lexical semantics, the present study included a larger number of participants (38), stimuli (50 per category), and image volumes (5,600) to increase statistical

power. We also improved on previous imaging studies of body part concept representation (Le Clec'H et al. 2000; Goldberg et al. 2006) by using fMRI methods with higher spatial and temporal resolution.

Participants

This study was initially intended to recruit 40 participants. Power analysis at the group level, where each participant is an individual sample, indicated that this sample size provides 80% power to detect effect sizes (Cohen's d) as small as 0.66 at 1-tailed alpha = 0.001. Ultimately, 45 participants were enrolled in the study, but 5 did not complete all scanning sessions, and 2 were excluded from the current analysis due to poor behavioral response consistency across stimulus repetitions (ICC <0.2). The final cohort comprised 38 adult native speakers of English (27 women, 11 men) with a mean age of 27 yr. All participants were right-handed according to the Edinburgh Handedness Scale (Oldfield 1971), had at least a high school education, and had no history of neurologic or psychiatric conditions. All participants gave written informed consent and were compensated for their time. The study was approved by the Medical College of Wisconsin Institutional Review Board.

To assess the adequacy of the sample size and experimental design, we conducted extensive retrospective analyses of reliability and RSA correlation magnitude as a function of sample size and number of stimulus repetitions using the present dataset (Mazurchuk et al. 2023). These analyses showed that both reliability and RSA magnitude reach an effective plateau at a sample size around 40 using the current experimental design with 6 stimulus repetitions. Doubling the sample size to 80 participants would only be expected to increase the mean RSA correlation from 0.49 to 0.53. Data from a subset of 25 participants in the present study were also previously analyzed and reported as "Experiment 2" in Tong et al. (2022). That analysis focused on demonstrating the multimodal nature of the representations in high order association cortices. Neither of these previous studies examined activation differences between object categories.

Stimuli and task

The complete stimulus set used in the fMRI study, described by Tong et al. (2022), consisted of 300 English nouns from 6 categories: animals, manipulable artifacts (hereafter "tools"), plants/foods, body parts, human traits, and quantities, with 50 words in each category. We focus here on the 4 concrete object categories (animals, tools, plants/foods, and body parts; see Table 1). Words were matched across these categories on letter and phoneme length, orthographic n-gram statistics, orthographic and phonologic neighborhood density, word frequency, word concreteness rating, lexical decision and naming accuracy, and lexical decision and naming reaction time. Values for these variables were obtained from the English Lexicon Project (Balota et al. 2007). Due to the diversity of items in the body part category, follow-up analyses were also performed using subsets of the body part category and are reported in the Supplementary Materials.

Scanning took place over the course of 3 sessions on separate days, with each session consisting of 6 runs, and each run consisting of 100 trials. On each trial, a noun was displayed in white font on a black background at the center of the screen for 500 ms, followed by a 2.5-s blank screen. Participants were instructed to rate each word on how often they encountered the corresponding entity in their daily life, using a scale from 1 ("rarely or never") to 3 ("often"). Responses were indicated using 3 keys operated with the right hand. Each trial was followed by a central

fixation cross with variable duration between 1 and 3 s (mean 1.5 s). Each run started and ended with an 8-s fixation cross. Stimulus presentation and response recording were performed with PsychoPy 3 software (Peirce et al. 2019) running on a Windows desktop computer with input from a Celeritas fiber optic response system (Psychology Software Tools, Inc.). Stimuli were displayed on an MRI-compatible liquid-crystal display screen positioned behind the scanner bore and viewed through a mirror attached to the head coil.

Semantic models

The model-based analyses used experiential (CREA) and distributional (Word2Vec) models of semantic content. The experiential representations for words were constructed from human ratings on 65 experiential domains (Binder et al. 2016). In brief, the experiential domains were selected based on known neural processing systems such as color, shape, visual motion, touch, audition, motor control, and olfaction, as well as other fundamental aspects of experience whose neural substrates are less clearly understood, such as space, time, affect, reward, numerosity, and others. As described previously (Binder et al. 2016), ratings were collected using the crowd sourcing tool Amazon Mechanical Turk to present a series of 65 queries about a target concept. Volunteers rated the relevance of each experiential domain to a given concept on a 0–6 Likert scale. For the purposes of RSA, the value of each feature, for each concept, was represented by averaging ratings across participants. This feature set was highly effective at clustering concepts into canonical taxonomic categories (e.g. animals, plants, vehicles, occupations, etc.; Binder et al. 2016) and has been used successfully to decode fMRI activation patterns during sentence reading (Anderson et al. 2016; Anderson et al. 2019). Previous comparisons with other semantic models, including WordNet, Word2Vec, and GloVe, showed that this experiential model is better at predicting neural similarity structure in the general semantic network, and that these other models do not add predictive power beyond that provided by the experiential model (Fernandino et al. 2022; Tong et al. 2022). The distributional model tested here, Word2Vec, creates vector representations of concepts by using a neural network to predict a masked word using the surrounding words (Mikolov et al. 2013). We used the pre-trained word embeddings accessed through the Python Gensim toolbox (Řehůřek and Sojka 2010).

Acquisition parameters

Images were acquired with a 3T GE Premier scanner at the Medical College of Wisconsin. Structural imaging included a T1-weighted (T1w) magnetization-prepared rapid acquisition with gradient echo volume (FOV = 256 mm, 222 axial slices, voxel size = $0.8 \times 0.8 \times 0.8$ mm) and a T2w CUBE acquisition (FOV = 256 mm, 222 sagittal slices, voxel size = $0.8 \times 0.8 \times 0.8$ mm). T2*-weighted gradient echo echo-planar images (EPI) were obtained for functional imaging using a simultaneous multi-slice (SMS) sequence (SMS factor = 4, TR = 1500 ms, TE = 33 ms, flip angle = 50°, FOV = 208 mm, 72 axial slices, in-plane matrix = 104 × 104, voxel size = $2 \times 2 \times 2$ mm). A pair of T2-weighted spin-echo echo planar scans (5 volumes each) with opposing phase-encoding directions was acquired before run 1, after run 3, and after run 6 to provide estimates of EPI geometric distortion in the phase-encoding direction.

Preprocessing

Images were preprocessed via a containerized version of the fMRIprep 22.0.1 pipeline (Esteban et al. 2019). The 3 T1w images

Table 1. Concrete object nouns used in the study.

Animal		Artifact		Body part		Plant–food	
Alligator	Hippopotamus	Anchor	Ladle	Abdomen	Lip	Apple	Eggplant
Baboon	Horse	Baseball	Magazine	Ankle	Liver	Asparagus	Grapes
Bird	Jackal	Binoculars	Microscope	Armpit	Muscle	Banana	Honey
Buffalo	Leopard	Bottle	Nail	Beard	Mustache	Beer	Lemon
Butterfly	Lion	Bowl	Pan	Belly	Navel	Bread	Lemonade
Camel	Monkey	Broom	Pencil	Bladder	Nipple	Broccoli	Milk
Cardinal	Moose	Calculator	Pipe	Cartilage	Nose	Butter	Mushroom
Cat	Mosquito	Camera	Rake	Cheek	Nostril	Cabbage	Mustard
Caterpillar	Mouse	Candle	Rope	Clavicle	Pancreas	Cake	Pear
Chameleon	Octopus	Cane	Ruler	Diaphragm	Pelvis	Carrot	Pineapple
Cheetah	Penguin	Cash	Saddle	Earlobe	Retina	Celery	Plant
Chicken	Pig	Comb	Sandpaper	Elbow	Shoulder	Cereal	Potato
Chimpanzee	Rabbit	Corkscrew	Scale	Eyebrow	Skeleton	Champagne	Pudding
Chipmunk	Rhinoceros	Crutches	Scissors	Eyelid	Skull	Cheese	Pumpkin
Cow	Salmon	Faucet	Screwdriver	Finger	Spine	Cherry	Raspberry
Cricket	Seal	Flashlight	Skillet	Fingernail	Stomach	Chestnut	Rice
Deer	Snail	Football	Spatula	Forearm	Testicle	Chocolate	Rose
Dog	Snake	Fork	Spoon	Forehead	Thigh	Cider	Sandwich
Dolphin	Spider	Glass	Stapler	Heel	Thumb	Coffee	Sauerkraut
Dragon	Squirrel	Hairbrush	Stethoscope	Instep	Toenail	Corn	Strawberry
Elephant	Tiger	Hammer	Thermometer	Intestines	Tooth	Cucumber	Sugar
Fish	Trout	Handsaw	Tongs	Kidney	Torso	Custard	Tangerine
Goat	Turkey	Iron	Towel	Knuckle	Trachea	Daisy	Tea
Goldfish	Turtle	Keyboard	Typewriter	Leg	Waist	Dandelion	Tobacco
Hamster	Whale	Knife	Umbrella	Ligament	Wrist	Egg	Tomato

(1 from each session) were corrected for intensity nonuniformity, and a T1w reference image was computed by averaging these images after registration using "mri_robust_template" (FreeSurfer 7.2.0). The T1w reference was then skull-stripped with a Nipype implementation of the "antsBrainExtraction.sh" workflow. Image segmentation into cerebrospinal fluid (CSF), white matter, and gray matter was performed on the skull-stripped T1w image using FAST (FSL 6.0.5). Brain surfaces were reconstructed using "recon-all" in FreeSurfer 7.2.0. The spin-echo images were used to estimate a B0-nonuniformity map using "topup" (FSL 6.0.5), which was used to unwarp the EPI data. For each of the EPI runs for each participant, a reference volume and its skull-stripped version were generated using fMRIprep. Head-motion parameters with respect to the EPI reference were estimated before any spatiotemporal filtering using MCFLIRT (FSL 6.0.5). EPI runs were slice-time corrected, and the EPI reference was coregistered to the T1w reference using "bbregister" (FreeSurfer), a boundary-based registration algorithm with 6 degrees of freedom. Grayordinate files using the fsLR-32k_midthickness cortical surface model (Glasser et al. 2013) containing 91 k samples were also generated using the highest resolution fsaverage as an intermediate standardized surface space. No additional spatial smoothing was applied.

Beta and *t*-values were calculated directly on the surface time-series data using 3dREMLFIT in AFNI (Cox 1996), incorporating 6 motion estimates, their derivatives, CSF and white matter regressors, and fourth order baseline polynomials for detrending. We separately z-scored response time estimates across each set of stimulus presentations and included them as nuisance regressors. Univariate category analysis used a REML model with 6 target regressors (1 for each category), and the EPI data were smoothed with a 6 mm full width at half maximum (FWHM) kernel. Multivariate analyses had no smoothing applied to the EPI data and used regression estimates derived from a REML model in which each word (involving all 6 presentations) was its own regressor.

In addition to the nuisance regressors, we censored volumes that had a framewise displacement greater than 0.9 mm.

Between-category comparisons

The analysis of category effects in the neural data is divided into 2 parts based on whether the analysis depends on an explicit model of semantic content.

Standard univariate analyses were performed to generate beta-maps for each of 4 categories (animals, tools, plants/foods, and body parts). Participant category beta-maps were then contrasted at the group level, and these pairwise differences were tested for significance at $P < 0.01$ using a Wilcoxon signed-rank test and false discovery rate (FDR) correction (Benjamini and Hochberg 1995) implemented in the python package "Statsmodels" (Seabold and Perktold 2010). To identify putative body part selective regions, we created a conjunction map of regions where body part activation was significantly greater than each of the other 3 categories. To aid in visualization, the conjunction analysis was restricted to clusters of at least 40 mm2.

To assess whether the main results were affected by inclusion of a broad range of items in the body part category, supplementary univariate conjunction analyses were also performed using subsets of words in the body part category (Supplementary Table S1). One possible factor in our stimulus set is whether the body parts are internal (e.g. liver) or external (e.g. nose). Another major division is between body parts that can be used as an effector and those that cannot be. To operationalize this latter distinction, we considered a body part to be a possible effector if it can be voluntarily moved in isolation. Lastly, the items were divided by general location into head, upper limb, torso, and lower limb. Supplementary Table S1 in the Supplementary materials lists these subcategory assignments for each item. Similar to the univariate analysis with all body parts, for each subcategory, conjunction analysis was performed relative to the 3 other concrete object

noun categories. In addition, words within each subcategory (e.g. internal and external) were directly contrasted.

MVPA analyses used surface-based "searchlight" regions of interest covering the entire cortical surface as well as vertex-wise *t*-values instead of beta-values. Searchlights were identical for the support vector machine (SVM) classifier, neural reliability, and RSA analyses. Searchlight patches were created using the Connectome Workbench toolbox (Marcus et al. 2011) as 10 mm radius circular surface areas defined on the HCP–fsLR-32 k midthickness surface.

The first MVPA consisted of training cross-validated SVM classifiers using all 6 pairs of the 4 object categories. To create an index of regions more selective for body parts, the 3 pairwise comparisons that included the body part category were averaged and compared to the average accuracy when body parts were not a target category. The rationale for this analysis is that information that is particularly relevant to body parts should be more useful for discriminating body part concepts from other object concepts than for discriminating between nonbody-part categories. We note that the SVM results are qualitative in nature; we opted for not estimating *P*-values using a binomial distribution because of evidence that the null distribution for cross-validated classifiers does not follow the binomial distribution (Noirhomme et al. 2014). A peak-finding algorithm was applied to the smoothed results (4 mm FWHM), in which extrema were required to be separated by at least 15 mm and have a minimum value of 0.07.

The second MVPA examined within-category reliability of the neural RDMs across participants for each category. Neural RDMs were calculated at the individual level using the Pearson correlation distance between the set of *t*-values within each surface patch. The reliability of these RDMs was calculated using the consistency–based ICC value. The ICC metric is related to standard noise ceiling measures but has the advantage of an associated framework for statistical interpretation. We note that ICC values are often interpreted based on ranges of the statistic (e.g. Cicchetti (1994) suggests that values between 0.60 and 0.74 be considered "good" agreement) rather than using *P*-values, and we therefore show the unthresholded statistic map so that patterns can be qualitatively compared to RSA maps. To determine whether there were regions that displayed body part *selectivity*, the reliability maps were contrasted between categories. Because there is no standard method for comparing ICC values with a repeated measures paradigm, we instead searched for vertices where the body part ICC value was above the range of the 99% confidence interval for each of the other 3 categories.

The third MVPA used model-dependent RSA to compare neural RDMs for each category with semantic model RDMs derived from either the 65-feature CREA model or Word2Vec. For RSA, similar to the within-category ICC analysis, we were interested in the qualitative pattern and therefore show the unthresholded RSA map. RSA using items restricted to 1 category indicates the regions involved in semantic representation of that category but does not speak to the preference of a region for a particular category. To parallel the approach taken in the univariate analysis, we used a Wilcoxon signed rank test on the paired differences between within-category RSA maps. The resulting *P*-values were FDR corrected and thresholded at *P* < 0.01. The *P*-value maps generated from this analysis were then eroded and dilated by 2 mm to smooth the results for visualization.

Encoding analysis

While a significant RSA correlation for a set of nouns from a particular category indicates that a semantic model captures the relevant relations *within* the category, it does not necessarily mean that the model accounts for differences between categories. That is, the hitherto described RSA does not address whether the semantic models explain activation differences *between* body parts and nonbody-part items. To test whether the semantic models can account for the mass univariate results, we performed a vertex-wise encoding analysis to generate predicted activation differences between body part words and other categories at each vertex, which were then compared to the observed differences. This analysis used 150 individual word beta maps from the nonbody-part conditions to predict beta maps for the left out 50 body part concepts. The encoding model was a ridge regression model that used leave-one-out cross-validation to determine the optimal penalty term on the training data. The 50 predicted maps were averaged across words and compared to the average of the 150 training words to determine the predicted contrast between body part and nonbody-part words for each participant. These differences were smoothed using a 6 mm FWHM Gaussian and tested against zero at each vertex using a Wilcoxon signed-rank test with significance set as FDR corrected *P*-values < 0.01.

Results

We group the analyses of neural data into semantic model independent and model dependent analyses. Performance on the familiarity judgment task during fMRI showed an excellent response rate of 97.5% and good intraindividual consistency across repeated presentations of the same word (mean ICC = 0.655).

The univariate conjunction analysis results in Fig. 1 show regions of cortex that are activated more for body part nouns compared to other concrete object noun categories. These regions included the left pMTG, left supramarginal gyrus (SMG), left precentral sulcus (preCS; including the premotor eye field [pEF]), left inferior frontal gyrus (IFG), and a small portion of the IPS (Table 2). In addition, there were small peaks in the left precuneus (preCun), left parainsular cortex (paraIns), and right pMTG.

Unthresholded maps that used subsets of the body part category showed similar results to the full set of stimuli and are reported in the Supplemental materials (Fig. S1 and S2). Subsets of external, internal, movable, and nonmovable were all found to be highly correlated with a conjunction created from the full set of body part words (Pearson r's = 0.97, 0.82, 0.93, 0.88, respectively). Direct comparison between external and internal groups showed increased activation in the left SMG for external body parts relative to internal body parts. Similarly, there was increased activation for movable relative to nonmovable body parts in bilateral SMG. While contrasts involving the other groups are discussed in the Supplementary materials, given the overall high similarity between subsets, all further results presented below are collapsed to the whole set to maximize power and generalizability.

The second analysis searched for regions of cortex where neural activation patterns discriminated body parts from other categories more than they did nonbody-part categories from each other (Fig. 1, bottom). Although qualitative in nature, the pattern is similar to that observed in the univariate analysis, with the largest peak differences located in the left SMG, left pMTG, left IFG, and left IPS (Table 2). In addition, there were small peaks in the left retrosplenial cortex (RSC), dorsal angular gyrus, preCS, and posterior middle frontal gyrus (pMFG).

Searchlight neural RDM reliability and RSA results for the body part category (Fig. 2, top row) showed a high degree of correspondence (Spearman rho across cortex: 0.801 for experiential model,
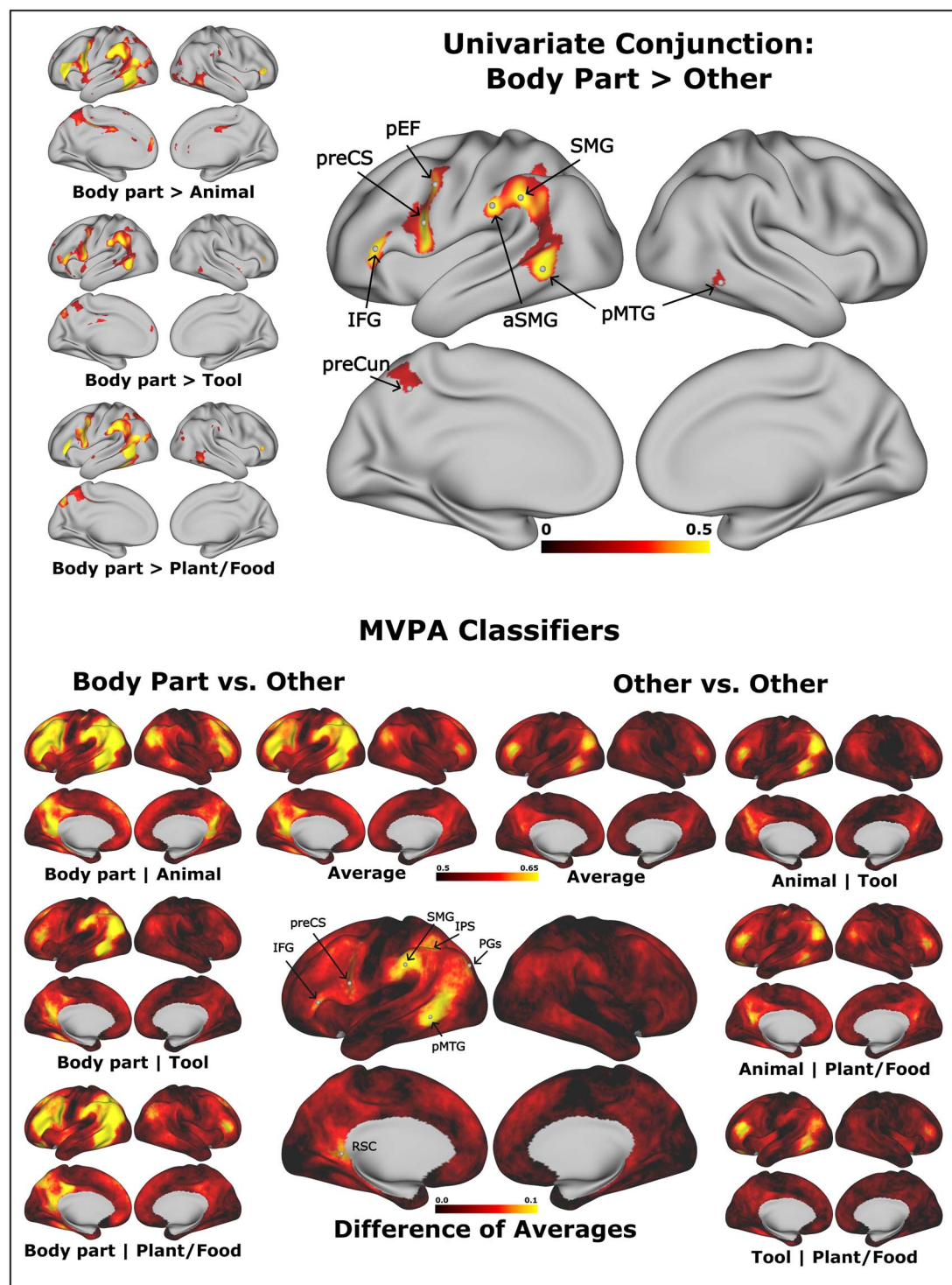
Fig. 1. Mass univariate and multivoxel pattern classifier analyses. Top: the top portion of the figure shows where blood-oxygen-level-dependent signal was greater for body part concepts than concepts from other categories based on standard mass univariate contrasts. All individual contrasts are significant at FDR corrected $P < 0.01$ using a 1-tailed Wilcoxon signed-rank test. The conjunction map shows where body parts produced greater activation in all comparisons. Colors in the individual comparisons represent average difference in beta-values. Bottom: the lower portion shows average classification accuracies for held out data in cross-validated searchlight SVM category classification. Classes were balanced, and 50% indicates chance accuracy. Shown in the center is the difference in average accuracy when one of the categories was body parts compared with when body parts are not a target category. Abbreviations are identified in the caption for Table 2.

0.807 for distributional model, and 0.963 between models). Peaks were found in the left pMTG, left SMG, left angular gyrus, left preCS, left posterior cingulate gyrus and preCun, and right IFG.

To examine the neural substrate of body part *specific* representations, we contrasted body part ICC and RSA maps to those

generated for other categories of nouns. In the case of the ICC analysis, body part selectivity was defined as regions where the ICC value for body parts was above the range of the ICC confidence interval for any other category. Peaks were found in the left pMTG, SMG, angular gyrus, preCS, and IFG, and several

Table 2. Peak coordinates corresponding to labels corresponding to the univariate analysis shown in Fig. 1. Coordinates refer to MNI 152 template space and parcel names are taken from the surface-based atlas in Glasser et al. (2016). For the univariate analysis, values correspond to the smallest bold difference between body parts and any other category. For the SVM analysis, values correspond to the average difference in cross-validated accuracy between category comparisons containing body parts, and category comparisons that do not contain body parts.

Analysis	Region	Coordinates (MNI)			Value at vertex	HCP parcel
Univariate	pMTG	−55	−56	−3	0.668	L_PHT
	preCS	−50	5	22	0.646	L_6r
	SMG	−60	−43	36	0.557	L_PF
	aSMG	−63	−27	30	0.538	L_Pfop
	IFG	−50	33	8	0.525	L_IFSa
	paraIns	−41	−6	−15	0.455	L_PI
	pEF	−46	−1	40	0.435	L_PEF
	IPS	−36	−50	38	0.404	L_IP2
	preCun	−7	−53	46	0.288	L_PCV
	pMTG	59	−53	−12	0.274	R_PHT
SVM	pMTG	−55	−55	−6	0.111	L_PHT
	SMG	−60	−35	35	0.107	L_PF
	IPS	−41	−46	41	0.101	L_IP2
	RSC	−9	−48	3	0.093	L_RSC
	IFG	−53	29	4	0.084	L_45
	PGs	−36	−82	34	0.081	L_PGs
	pMFG	−28	16	48	0.081	L_8Av
	preCS	−52	6	20	0.079	L_6r

IFG = inferior frontal gyrus, IPS = intraparietal sulcus, paraIns = parainsular cortex, pEF = premotor eye field, PGs = superior part of Von Economo and Koskinas area PG, pMFG = posterior middle frontal gyrus, pMTG = posterior middle temporal gyrus, preCS = precentral sulcus, preCun = precuneus, RSC = retrosplenial cortex, SMG = supramarginal gyrus.

homologous regions in the right hemisphere. For the RSA contrasts, paired difference contrast maps were generated for body parts relative to the other 3 categories. A conjunction map was then generated indicating the vertices where RSA values were significantly higher for body parts than for all other categories as assessed by an FDR corrected P-value < 0.01 derived from a Wilcoxon signed-rank test. RSA contrasts using the 2 semantic models produced similar results. Both models had significant vertices in the left pMTG, SMG, posterior angular gyrus, and preCun.

Finally, we tested whether semantic models could predict the body part selective regions found in univariate analysis by way of a vertex-wise encoding analysis. Unthresholded predicted maps resembled the observed maps using both the experiential and the distributional model (Fig. 3), though the vertex-wise correlation between predicted and observed maps was higher for the experiential model (Spearman rho = 0.400 for experiential, 0.203 for distributional). The experiential model captured most of the features of the observed map, except for the higher activation for body parts in left inferior frontal cortex and the higher activation for nonbody-part concepts in posterior left ventral temporal regions. Statistical significance was assessed at each vertex using a Wilcoxon signed-rank test across all participants and using a threshold of FDR corrected P-values < 0.01. Both models replicated the observed significant differences between body parts and other words in left pMTG and left angular gyrus. The experiential model better replicated clusters in the SMG and preCun, whereas the distributional model better replicated clusters in the left IFG, preCS, and posterior inferior temporal gyrus.

Discussion

Several complementary analyses were conducted to identify the neural substrates of body part word processing relative to other object categories. One region, the left pMTG, appeared in all analyses, indicating an important role for this region in preferential body part semantic representation. Broadly, the univariate analysis highlighted 3 regions: left pMTG, left SMG, and left preCS. These 3 regions also appeared in the SVM classifier analysis, the body part neural RDM reliability analysis, and the RSA results, although only the left pMTG and SMG showed higher RSA values for body parts compared to other categories. The model-based encoding analyses also predicted body part vs other category differences in these 3 regions, though with some differences between the models. The close agreement between the reliability map and RSA results in Fig. 2 indicates that both semantic models successfully capture shared variance across much of the cortex and gives support to the validity of the underlying semantic models. The reliability and RSA contrasts between categories identified similar regions to those that appeared in the univariate analysis, indicating converging evidence for the involvement of the relevant regions in body part representation.

The pMTG has been implicated in a variety of functions (Hodgson et al. 2022), and this general region appears to be composed of several functionally and anatomically distinct sub-regions (Glasser et al. 2016). As shown in Fig. 4a, the multimodal cortical parcellation created by the Human Connectome Project (HCP) divides the pMTG into distinct regions, including, from more anterior to posterior: TE1p, PHT, PH (which extends into posterior inferior temporal gyrus), and FST (Glasser et al. 2016). Notably, the pMTG region most strongly activated by body part words relative to other categories in our univariate analyses aligns quite closely with area PHT (Fig. 4b). The HCP dataset also provides an opportunity to compare our results with a previously described "extrastriate body area" (EBA) that shows stronger activation to body part images than to other categories of objects (Downing et al. 2001; Downing et al. 2006; Orlov et al. 2010), as this dataset includes activation maps produced by contrasting object *pictures* from different categories, including body part images, during an n-back working memory task (Barch et al. 2013). As shown in Fig. 4c, the region of strongest selectivity for body part images is
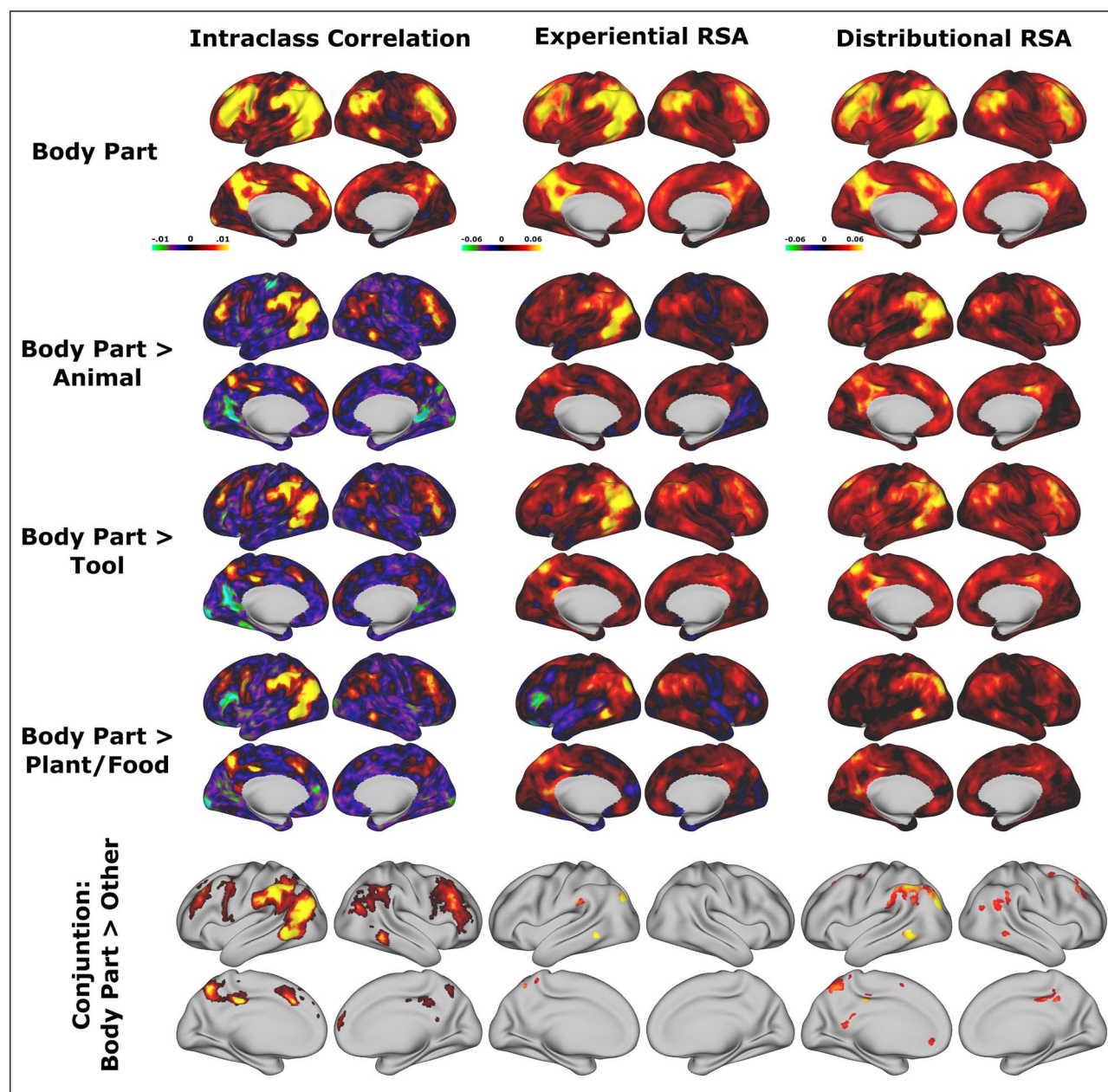
Fig. 2. ICC and RSA comparisons. ICC and RSA maps were generated for each of 4 categories of nouns. Results for the body part category are shown in the top row, and contrasts between body part and other categories are shown in subsequent rows. The bottom row shows conjunction maps of the categorical comparisons. Colors in the ICC conjunction map represent the difference between the body part ICC value and the highest upper limit of the confidence interval for any of the other 3 categories. The RSA conjunction maps were generated by testing the mean of paired differences against zero using a Wilcoxon signed-rank test. The conjunction maps show vertices where body part RSA values were larger than for any other category using an FDR corrected $P < 0.01$ threshold. The conjunction map color shows the mean paired difference between body part RSA values and whichever other category had the highest RSA value for that vertex.

largely posterior to PHT, involving areas FST, TPOJ2, and several extrastriate parcels surrounding the MT complex (V4t, LO3, and TPOJ3), although there is also involvement of the posterior aspect of PHT. This proximity between areas showing category preferences for images and category preferences for words is consistent with a longstanding view of cortical organization in which sensory processing streams represent information in increasingly conjunctive and abstract form with greater distance from primary cortex (Damasio 1989; Tanaka 1996; Mesulam 1998; Simmons and Barsalou 2003). Recent work by Popham et al. (2021) provides similar evidence that visually- and verbally-elicited

representations of object categories are aligned spatially near the occipitotemporal border, with verbally-elicited representations immediately anterior to representations elicited by object pictures (Orlov et al. 2010).

Similarly, the SMG has been divided into several subregions based on anatomical and functional characteristics (Caspers et al. 2006; Caspers et al. 2008; Glasser et al. 2016). Our univariate contrasts of body part words compared to other categories produced activation peaks in areas PF and PFop of the HCP parcellation, though activation also involved portions of PFm, PSL, and PGi. Interestingly, the contrast of body part pictures vs other categories
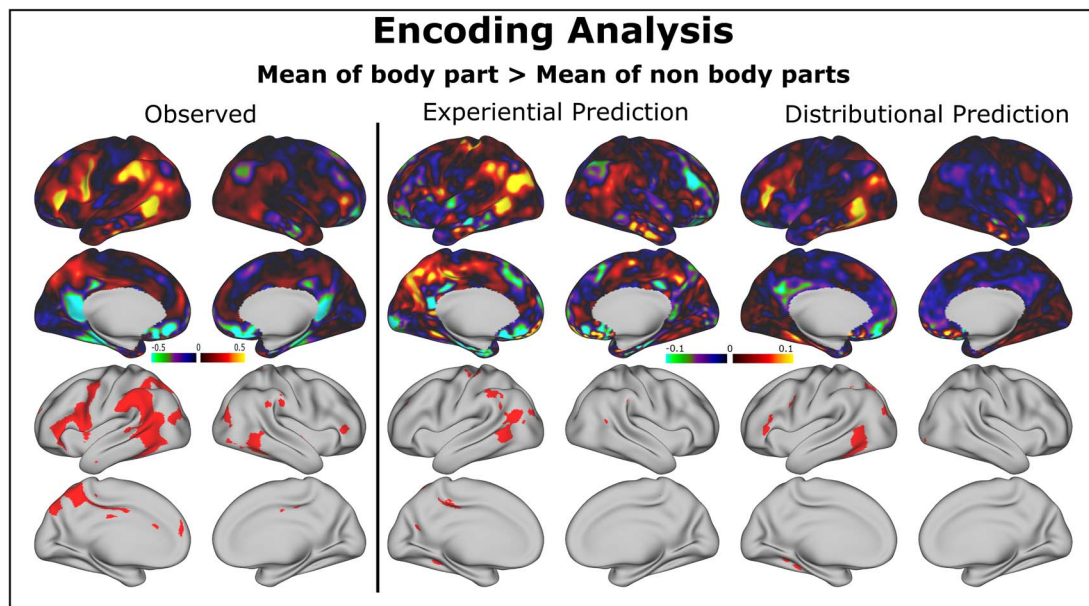
Fig. 3. Vertex–wise encoding results. Shown on the left is the difference between the average of all body part concepts and average of all other concrete concepts. On the right is the result of a vertex–wise encoding model trained on 150 concrete concepts to predict beta values for the 50 body part concepts. Shown is the average difference between the average of the 50 predicted values and the 150 observed values along with vertices that were significantly larger for body parts at FDR corrected $P < 0.01$ using a 1-tailed Wilcoxon signed-rank test.

in the HCP dataset also produces activation in this region (Fig. 4c), but the center of mass of this activation is somewhat anterior to the activation cluster produced by body part words in our data. The 2 studies share a peak in the posterior aspect of PFop, but the highest peak for body part words is in posterior PF, with activation spreading more posteriorly into PFm, PSL, and PGi, none of which are activated by body part images. Body part images also activate the anterior parietal area PFt, a region not selectively activated by body part words. This partially overlapping anterior–posterior gradient is reminiscent of the posterior–anterior gradient observed in pMTG, in that body part words selectively activate cortical regions more distant from primary sensory cortex, in this case somatosensory cortex (Iwamura 1998), compared to body part images (Fig. 4d).

The third region engaged selectively by body part words was the preCS, which has also been divided into several subregions. The largest cluster aligns very closely with HCP region 6r, which is in the rostral bank of the lower preCS. Other precentral areas activated were area pEF just superior to 6r, and area 55b superior to pEF. These regions comprise rostral premotor cortex; they lie adjacent to but "upstream" from primary motor cortex. Apart from weak activation of area 6r, these regions were not activated by body part images compared to other categories in the HCP dataset. A final activation cluster related to body part words straddled HCP areas IFSa and 45 in the pars triangularis of the IFG. The significance of this region is corroborated by the findings of Kemmerer and Tranel (2008), who reported that, among the 9 patients with left hemisphere damage and impaired naming of body parts, 8 displayed the highest degree of lesion overlap in the frontal opercular cortex.

The network of regions activated by body part words relative to other categories is remarkably recapitulated by a seed-based connectivity analysis of the HCP "resting state" fMRI dataset using area PHT as seed (Fig. 4e). This suggests that these regions form a cohesive functional network with PHT, PF, and 6r among its principal nodes. A similar or identical network has been extensively implicated in action performance and action observation (Caspers et al. 2010; Rizzolatti and Sinigaglia 2010; Grosbras et al. 2012), except that the network activated by action performance/observation is typically bilateral and symmetric, whereas the body part word network is strongly left-lateralized. In keeping with an embodied cognition perspective, we propose that this left hemisphere network of high-level association cortices supports the retrieval of body part concepts through partial activation of relevant multimodal experiential information, including the visual shapes, sizes, and movements of body parts; tactile, proprioceptive, and relative spatial location information supporting the body schema and body structural description; and motor programs associated with particular body parts and object-directed actions. Based solely on their spatial proximity to different sensory–motor systems, we hypothesize that the SMG component of the network (areas PF and PFop) plays a larger role in retrieving somatosensory information relevant to the body schema and body structural description, whereas the pMTG node has a larger role in retrieving visual shape and visual motion information, and the preCS a larger role in retrieving information about motor programs associated with certain body parts.

Evidence from lesion studies provides some support for these distinctions. Vascular lesions involving the EBA (Moro et al. 2008) and repetitive transcranial magnetic stimulation applied to the EBA (Urgesi et al. 2004; Urgesi et al. 2007) are associated with selective impairments of body part visual form discrimination without impairment of body part action discrimination. In contrast, Moro et al. (2008) found evidence linking body part action discrimination to ventral premotor cortex and posterior IFG in a lesion-symptom mapping study of 28 patients with vascular lesions. Damage in this region produced larger deficits on a body part action discrimination task compared to a body part form discrimination task. Damage to anterior parietal somatosensory cortex has long been linked with impairments of touch and haptic perception, including impairments of touch localization (atopognosia) believed to reflect damage to a "superficial body schema" (Head and Holmes 1911; Critchley 1953; Longo et al. 2010). Somatosensory inputs also provide dynamic proprioceptive
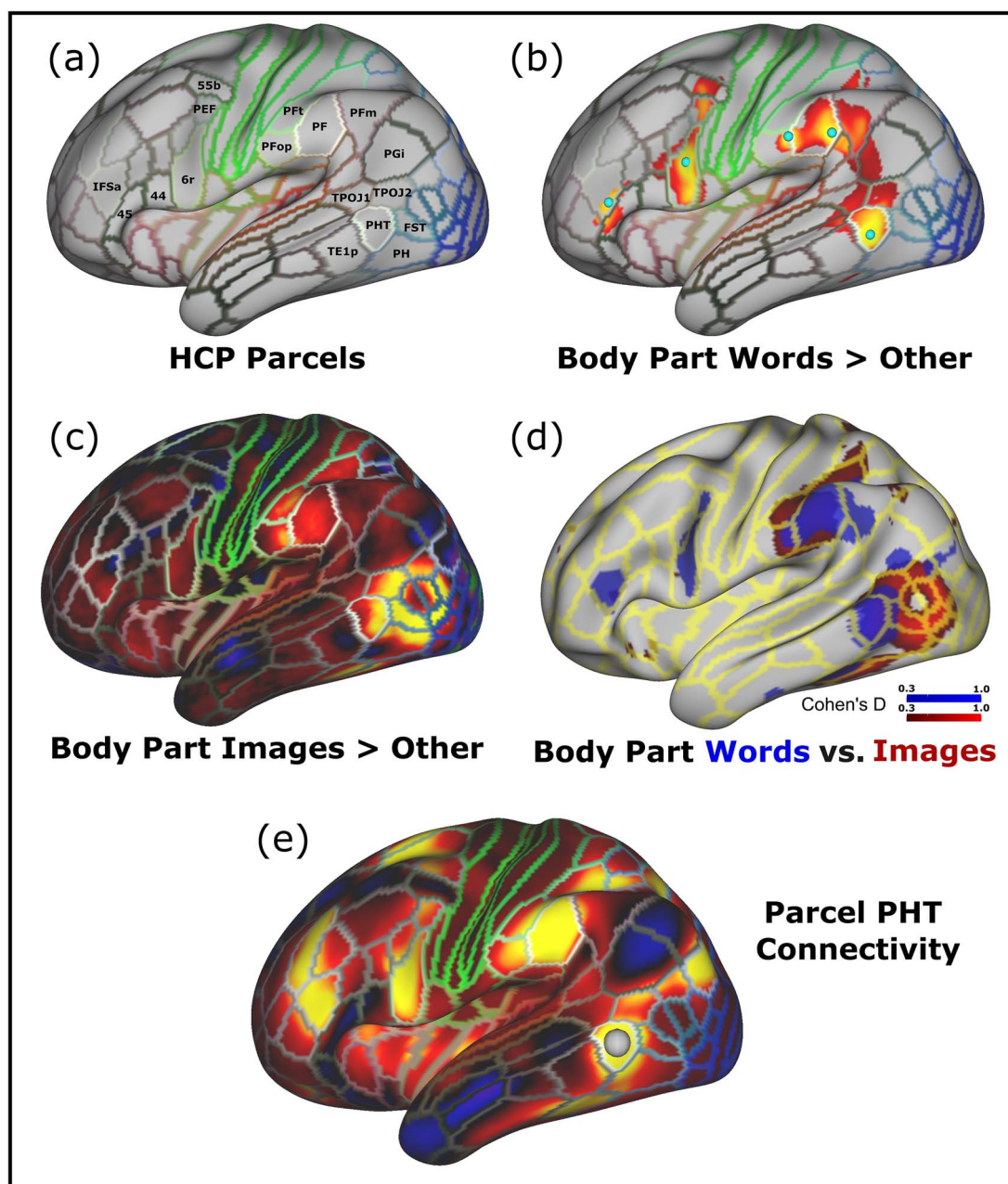
Fig. 4. a) Select HCP parcels are labeled. The coloring corresponds to that used in the original report by Glasser et al. (2016). b) Body part word > other category univariate results overlaid with HCP parcel boundaries. c) Body part pictures > other category during a working memory task, univariate results from the HCP dataset. d) Overlap of the maps generated by body part words relative to other categories in the current study and body part images relative to other categories in the HCP dataset. The current results are displayed in Cohen's D units, the same units as the HCP data, and thresholded so that only values greater than 0.3 are displayed for both maps. e) Resting-state fMRI connectivity map using seed-based correlation, with a seed placed in left PHT applied to data from 1003 participants in the HCP S1200 release.

information that allows representation of body part positions and postures via a "postural schema" that stores knowledge about the dimensions of body parts (Longo et al. 2010). Schwoebel and Coslett (2005) tested patients on their ability to perform imagined hand movements and to judge the laterality (left or right) of visually presented hand pictures, both of which the authors considered to depend on these dynamic somatosensory representations of the body. Patients with deficits on these tasks tended to have lesions involving either the left or right SMG.

Notably, the SMG showed greater selective body part activation in the current study for body parts that are external or movable compared to those that are internal or not movable. This finding

is consistent with the claim that the SMG supports a dynamic somatosensory representation of the body, in that neither internal nor spatially fixed body parts would be expected to have a dynamic somatosensory representation. That is, internal body parts cannot be touched and so have no superficial body schema, and immobile body parts do not change position and so have little proprioceptive or postural representation.

Most relevant for identifying the critical substrate for a *spatial* representation of the body are studies of individuals with autotopagnosia. Patients with this rare disorder are unable to locate named body parts either on their own or other bodies, but typically can name individual body parts and describe their

function (Pick 1922), suggesting specific damage to a spatial structural description of the body (Buxbaum and Coslett 2001). Some patients with autotopagnosia have had relatively diffuse vascular or neurodegenerative lesions (Pick 1922; Sirigu et al. 1991; Buxbaum and Coslett 2001). Those with focal damage have tended to have left parietal lobe lesions (Ogden 1985; Semenza 1988; Denes et al. 2000; Schwoebel et al. 2001; Guariglia et al. 2002), although Schwoebel and Coslett (2005) observed a marginally higher frequency of damage in the temporal lobe than in the parietal lobe in patients who were impaired on body part localization tests.

Other evidence on parietal lobe involvement in body part spatial representation comes from 2 functional imaging studies. Le Clec'H et al. (2000) reported activation in the left IPS and several left frontal regions during a spatial judgment task on body part names ("Is it above or below the shoulders?") compared to a size judgment task on numbers ("Is it less than 12?"). The lack of comparison with other body part tasks in this study, however, leaves open the question of whether these activations are specific to the spatial judgment task. Corradi-Dell'Acqua et al. (2008) compared tasks requiring either relative distance judgment or name retrieval with pairs of body part or building part images. A focus in the left posterior IPS showed stronger activation for the distance judgment task than the name retrieval task, but only for body parts, suggesting selective processing of body part location information in this area. We observed evidence for selective involvement of anterior portions of the IPS (HCP parcels AIP and IP2) in body part word processing in the univariate contrast, classifier, and intraclass correlation analyses (Fig. 1 and 2). The IPS was also implicated in the semantic representation of body parts by a prior study that used body part images and whole-brain searchlight RSA with a distributionally-derived semantic model (Bracci et al. 2015), although those authors did not compare activation in the IPS for body parts relative to other categories.

Other evidence suggests that the pMTG may also store more abstract semantic knowledge related to body parts. Schwoebel and Coslett (2005) found 16 patients (among a sample of 70) who had deficits on matching body parts by function and matching body parts to associated clothing and objects, both tasks designed to assess higher-level semantic knowledge about body parts. Of the 13 with available imaging data, 12 had lesions involving the temporal lobe. Three of these had deficits confined to these semantic measures, without impairment on lower-level body schema (action imagery and hand laterality judgments) or body part localization tasks, and the lesions in these patients overlapped mainly in the left posterior temporal lobe. The pMTG (MNI: −57, −54, −10) was also implicated in the semantic representation of body parts in the study by Bracci et al. (2015).

Studies on regions involved in the semantic processing of verbs have also repeatedly implicated the pMTG and surrounding area. There is an inherent connection between body parts and verbs given that actions are performed using body parts. An activation likelihood estimation meta-analysis (Faroqi-Shah et al. 2018) of 23 studies contrasting verb vs noun processing (33 contrasts, 190 activation foci) showed a reliable activation cluster for verbs greater than nouns in the left pMTG (MNI: −56, −46, 7) near our reported peak, as well as smaller clusters in left IFG (MNI: −42, 21, 5) and pEF (MNI: −48, 6, 40) close to those observed in our univariate analysis. Thus, the network we associate with preferential processing of body part knowledge overlaps to a large extent with the network of regions previously implicated in verb > noun processing. Motion is also an intrinsic component of many verb concepts. A study on the representation of verbs found

that of 5 verb classes containing a motion component, all had overlapping activation in the posterior lateral temporal cortex (Fig. 3; Kemmerer et al. 2008). Given the inherent correlations between body part concepts, actions represented by verbs, and motion content of verbs, comparing the differential contributions of these knowledge types to activation in these regions will be challenging. It seems likely to us that this network represents all of these inter-related forms of knowledge, which collectively contribute to our understanding of body movements and body–object interactions.

The data in Goodglass et al. (1966) and a thorough review by Capitani et al. (2003) of reported category-selective deficits indicate typical sparing of body part knowledge relative to other categories of concrete object concepts in brain-damaged individuals. There are at least 3 possible reasons for this typical sparing. First, the evidence presented by Schwoebel and Coslett (2005) suggests that the pMTG and adjacent posterior ITG may be the most critical zone for supporting body part concepts. This zone lies at the posterior edge of the middle cerebral artery territory and is often spared in stroke. A second possibility is that body part concepts may have a more distributed (i.e. redundant) representation compared to other categories and thus be more resilient to focal damage. Finally, many body part concepts (e.g. hand, arm, leg, head, mouth, eye, and nose) are acquired at an early age and are highly familiar. Body part knowledge might therefore appear to be more resilient to brain damage when items are not matched on these variables. These accounts are not mutually exclusive, and all may be true to some degree. Our results favor a key role for the preferential representation of body parts in the left pMTG, consistent with the lesion evidence implicating this region (Schwoebel and Coslett 2005).

We observed body part > other category effects in the left preCS in several model free analyses (univariate contrasts, classifier contrasts, and neural RDM reliability contrasts) that does not appear to be well accounted for in the semantic models, as it did not show a significant category effect in RSA and only weakly in the encoding results. This could potentially be the result of a feature or set of features being represented in this region but not accounted for in the semantic models. Alternatively, the features represented in this region might be as relevant for distinguishing between members of other categories as they are for distinguishing body parts, resulting in RSA values for 1 of the other categories that are as high as for body parts. For example, if this region mainly represents motor programs associated with actions, as we hypothesize, then it may be just as important for representing the similarity structure among tool concepts (which differ markedly in the actions associated with their use) as the similarity structure among body part concepts.

Defining category effects on brain activation patterns entails comparisons between categories, and the results naturally depend on the range and specific type of categories that are included for comparison. A limitation of the current study is that it involved just 4 categories, leaving open the possibility that some other category might exist that activates the identified areas as much as body part words. We believe this is unlikely given that 2 of the categories we included—tools and food/plants—are associated with object-directed actions and thus conceptually related to body parts, and the tool category, in particular, is known to preferentially activate closely adjacent or overlapping regions of the pMTG. In addition, many exemplars in the animal category have body part features (head, mouth, eyes, arm, leg, torso, etc.) not dissimilar from human body parts. Another general limitation of fMRI studies is the variety of analysis techniques

available and the inherent degrees of freedom this introduces. We believe our study mitigates this by focusing on the convergent results across four very different analysis approaches. Given that the regions we identified showed stronger responses to body part words in comparison to other categories across all these analyses, and given the salience of body parts to many aspects of daily life, we believe the present evidence supports the claim for a brain network that is relatively specialized for representing body part knowledge. Future research should examine comparisons between body part concepts and a wider variety of other categories.

Conclusion

Our results show that lexical-semantic representations of body parts are distributed in a multilobar, left-lateralized network primarily involving posterior temporal, inferior parietal, and precentral cortex. Two commonly-used models of semantic content accounted for within-category representational geometry and for univariate contrasts implicating the pMTG and SMG in body part representation. The results are broadly consistent with available neuropsychological evidence from individuals with focal brain damage and contribute to a developing mechanistic account of body part knowledge impairments.

Acknowledgments

The authors thank Samantha Hudson, Sidney Schoenrock, and Jed Mathis for help with data collection, and Joseph Heffernan for help with data analysis.

Author contributions

Stephen Mazurchuk (Data curation, Formal analysis, Methodology, Visualization, Writing—original draft, Writing—review & editing), Leonardo Fernandino (Conceptualization, Methodology, Writing—review & editing), Jia-Qing Tong (Methodology, Writing—review & editing), Lisa L. Conant (Methodology, Validation), and Jeffrey R. Binder (Conceptualization, Funding acquisition, Methodology, Project administration, Resources, Supervision, Visualization, Writing—review & editing).

Supplementary material

Supplementary material is available at *Cerebral Cortex* online.

References

Anderson A, Binder JR, Fernandino L, Humphries CJ, Conant LL, Aguilar M, Wang X, Doko D, Raizada RDS. Predicting neural activity patterns associated with sentences using a neurobiologically motivated model of semantic representation. *Cereb Cortex*. 2016:27(9):4379–4395. https://doi.org/10.1093/cercor/bhw240.

Anderson AJ, Binder JR, Fernandino L, Humphries CJ, Conant LL, Raizada RDS, Lin F, Lalor EC. An integrated neural decoder of linguistic and experiential meaning. *J Neurosci*. 2019:39(45):8969–8987. https://doi.org/10.1523/JNEUROSCI.2575-18.2019.

Balota DA, Yap MJ, Hutchison KA, Cortese MJ, Kessler B, Loftis B, Neely JH, Nelson DL, Simpson GB, Treiman R. The English lexicon project. *Behav Res Methods*. 2007:39(3):445–459. https://doi.org/10.3758/BF03193014.

Barch DM, Burgess GC, Harms MP, Petersen SE, Schlaggar BL, Corbetta M, Glasser MF, Curtiss S, Dixit S, Feldt C, et al. Function in the human connectome: task-fMRI and individual differences in behavior. *NeuroImage*. 2013:80(15 October):169–189. https://doi.org/10.1016/j.neuroimage.2013.05.033.

Benjamini Y, Hochberg Y. Controlling the false discovery rate: a practical and powerful approach to multiple testing. *J R Stat Soc Series B Stat Methodology*. 1995:57(1):289–300. https://doi.org/10.1111/j.2517-6161.1995.tb02031.x.

Binder JR, Conant LL, Humphries CJ, Fernandino L, Simons SB, Aguilar M, Desai RH. Toward a brain-based componential semantic representation. *Cogn Neuropsychol*. 2016:33(3–4):130–174. https://doi.org/10.1080/02643294.2016.1147426.

Boccia M, Raimo S, Vita AD, Battisti A, Matano A, Guariglia C, Grossi D, Palermo L. Topological and hodological aspects of body representation in right brain damaged patients. *Neuropsychologia*. 2020:148(Nov):107637. https://doi.org/10.1016/j.neuropsychologia.2020.107637.

Bracci S, Caramazza A, Peelen MV. Representational similarity of body parts in human occipitotemporal cortex. *J Neurosci*. 2015:35(38):12977–12985. https://doi.org/10.1523/JNEUROSCI.4698-14.2015.

Buxbaum LJ, Coslett HB. Specialised structural descriptions for human body parts: evidence from autotopagnosia. *Cogn Neuropsychol*. 2001:18(4):289–306. https://doi.org/10.1080/02643290126172.

Capitani E, Laiacona M, Mahon B, Caramazza A. What are the facts of semantic category-specific deficits? A critical review of the clinical evidence. *Cogn Neuropsychol*. 2003:20(3–6):213–261. https://doi.org/10.1080/02643290244000266.

Caspers S, Geyer S, Schleicher A, Mohlberg H, Amunts K, Zilles K. The human inferior parietal cortex: cytoarchitectonic parcellation and interindividual variability. *NeuroImage*. 2006:33(2):430–448. https://doi.org/10.1016/j.neuroimage.2006.06.054.

Caspers S, Eickhoff SB, Geyer S, Scheperjans F, Mohlberg H, Zilles K, Amunts K. The human inferior parietal lobule in stereotaxic space. *Brain Struct Funct*. 2008:212(6):481–495. https://doi.org/10.1007/s00429-008-0195-z.

Caspers S, Zilles K, Laird AR, Eickhoff SB. ALE meta-analysis of action observation and imitation in the human brain. *NeuroImage*. 2010:50(3):1148–1167. https://doi.org/10.1016/j.neuroimage.2009.12.112.

Cicchetti DV. Guidelines, criteria, and rules of thumb for evaluating normed and standardized assessment instruments in psychology. *Psychol Assess*. 1994:6(4):284–290. https://doi.org/10.1037/1040-3590.6.4.284.

Corradi-Dell'Acqua C, Hesse MD, Rumiati RI, Fink GR. Where is a nose with respect to a foot? The left posterior parietal cortex processes spatial relationships among body parts. *Cereb Cortex*. 2008:18(12):2879–2890. https://doi.org/10.1093/cercor/bhn046.

Cox RW. AFNI: software for analysis and visualization of functional magnetic resonance neuroimages. *Comput Biomed Res*. 1996:29(3):162–173. https://doi.org/10.1006/cbmr.1996.0014.

Critchley M. *The parietal lobes*. Oxford, England: Williams and Wilkins; 1953.

Damasio AR. Time-locked multiregional retroactivation: a systems-level proposal for the neural substrates of recall and recognition. *Cognition*. 1989:33(1–2):25–62. https://doi.org/10.1016/0010-0277(89)90005-X.

Denes G, Cappelletti JY, Zilli T, Porta FD, Gallana A. A category-specific deficit of spatial representation: the case of autotopagnosia. *Neuropsychologia*. 2000:38(4):345–350. https://doi.org/10.1016/S0028-3932(99)00101-3.

Downing PE, Jiang Y, Shuman M, Kanwisher N. A cortical area selective for visual processing of the human body. *Science*. 2001:293(5539):2470–2473. https://doi.org/10.1126/science.1063414.

Downing PE, Peelen MV, Wiggett AJ, Tew BD. The role of the extrastriate body area in action perception. *Soc Neurosci*. 2006:1(1):52–62. https://doi.org/10.1080/17470910600668854.

Esteban O, Markiewicz CJ, Blair RW, Moodie CA, Isik IA, Erramuzpe A, Kent JD, Goncalves M, DuPre E, Snyder M, et al. fMRIPrep: a robust preprocessing pipeline for functional MRI. *Nat Methods*. 2019:16(1):111–116. https://doi.org/10.1038/s41592-018-0235-4.

Faroqi-Shah Y, Sebastian R, Woude AV. Neural representation of word categories is distinct in the temporal lobe: an activation likelihood analysis. *Hum Brain Mapp*. 2018:39(12):4925–4938. https://doi.org/10.1002/hbm.24334.

Fernandino L, Tong J-Q, Conant LL, Humphries CJ, Binder JR. Decoding the information structure underlying the neural representation of concepts. *Proc Natl Acad Sci USA*. 2022:119(6):e2108091119. https://doi.org/10.1073/pnas.2108091119.

Gainotti G. A metanalysis of impaired and spared naming for different categories of knowledge in patients with a visuo-verbal disconnection. *Neuropsychologia*. 2004:42(3):299–319. https://doi.org/10.1016/j.neuropsychologia.2003.08.006.

Glasser MF, Sotiropoulos SN, Wilson AJ, Coalson TS, Fischl B, Andersson JL, Xu J, Jbabdi S, Webster M, Polimeni JR, et al. The minimal preprocessing pipelines for the human connectome project. *NeuroImage*. 2013:80(15 Oct):105–124. https://doi.org/10.1016/j.neuroimage.2013.04.127.

Glasser MF, Coalson TS, Robinson EC, Hacker CD, Harwell J, Yacoub E, Ugurbil K, Andersson J, Beckmann CF, Jenkinson M, et al. A multi-modal parcellation of human cerebral cortex. *Nature*. 2016:536(7615):171–178. https://doi.org/10.1038/nature18933.

Goldberg RF, Perfetti CA, Schneider W. Distinct and common cortical activations for multimodal semantic categories. *Cogn Affect Behav Neurosci*. 2006:6(3):214–222. https://doi.org/10.3758/CABN.6.3.214.

Goodglass H, Klein B, Carey P, Jones K. Specific semantic word categories in aphasia. *Cortex*. 1966:2(1):74–89. https://doi.org/10.1016/S0010-9452(66)80029-1.

Grosbras MH, Beaton S, Eickhoff SB. Brain regions involved in human movement perception: a quantitative voxel-based meta-analysis. *Hum Brain Mapp*. 2012:33(2):431–454. https://doi.org/10.1002/hbm.21222.

Guariglia C, Piccardi L, Allegra MCP, Traballesi M. Is autotopoagnosia real? EC says yes. A case study. *Neuropsychologia*. 2002:40(10):1744–1749. https://doi.org/10.1016/S0028-3932(02)00013-1.

Head H, Holmes G. Sensory disturbances from cerebral lesions. *Brain*. 1911:34(2–3):102–254. https://doi.org/10.1093/brain/34.2-3.102.

Hodgson VJ, Lambon Ralph MA, Jackson RL. The cross-domain functional organization of posterior lateral temporal cortex: insights from ale meta-analyses of 7 cognitive domains spanning 12,000 participants. *Cereb Cortex*. 2022:33(8):4990–5006. https://doi.org/10.1093/cercor/bhac394.

Iwamura Y. Hierarchical somatosensory processing. *Curr Opin Neurobiol*. 1998:8(4):522–528. https://doi.org/10.1016/S0959-4388(98)80041-X.

Jastorff J, Begliomini C, Fabbri-Destro M, Rizzolatti G, Orban GA. Coding observed motor acts: different organizational principles in the parietal and premotor cortex of humans. *J Neurophysiol*. 2010:104(1):128–140. https://doi.org/10.1152/jn.00254.2010.

Kemmerer D, Tranel D. Searching for the elusive neural substrates of body part terms: a neuropsychological study. *Cogn Neuropsychol*. 2008:25(4):601–629. https://doi.org/10.1080/02643290802247052.

Kemmerer D, Castillo JG, Talavage T, Patterson S, Wiley C. Neuroanatomical distribution of five semantic components of verbs: evidence from fMRI. *Brain Lang*. 2008:107(1):16–43. https://doi.org/10.1016/j.bandl.2007.09.003.

Kriegeskorte N, Mur M, Bandettini PA. Representational similarity analysis—connecting the branches of systems neuroscience. *Front Syst Neurosci*. 2008:2(24 Nov):4. https://doi.org/10.3389/neuro.06.004.2008.

Laiacona M, Allamano N, Lorenzi L, Capitani E. A case of impaired naming and knowledge of body parts. Are limbs a separate sub-category? *Neurocase*. 2006:12(5):307–316. https://doi.org/10.1080/13554790601125940.

Le Clec'H G, Dehaene S, Cohen L, Mehler J, Dupoux E, Poline JB, Lehéricy S, Moortele PFvd, Bihan DL. Distinct cortical areas for names of numbers and body parts independent of language and input modality. *NeuroImage*. 2000:12(4):381–391. https://doi.org/10.1006/nimg.2000.0627.

Lingnau A, Downing PE. The lateral occipitotemporal cortex in action. *Trends Cogn Sci*. 2015:19(5):268–277. https://doi.org/10.1016/j.tics.2015.03.006.

Longo MR, Azañón E, Haggard P. More than skin deep: body representation beyond primary somatosensory cortex. *Neuropsychologia*. 2010:48(3):655–668. https://doi.org/10.1016/j.neuropsychologia.2009.08.022.

Marcus DS, Harwell J, Olsen T, Hodge M, Glasser MF, Prior F, Jenkinson M, Laumann T, Curtiss SW, Van Essen DC. Informatics and data mining tools and strategies for the human connectome project. *Front Neuroinform*. 2011:5(27 Jun):4. https://doi.org/10.3389/fninf.2011.00004.

Mazurchuk S, Conant LL, Tong J-Q, Binder JR, Fernandino L. Stimulus repetition and sample size considerations in item-level representational similarity analysis. *Lang Cogn Neurosci* (ahead-of-print). 2023:1–12. https://doi.org/10.1080/23273798.2023.2232903.

Mesulam MM. From sensation to cognition. *Brain*. 1998:121(6):1013–1052. https://doi.org/10.1093/brain/121.6.1013.

Mikolov T, Chen K, Corrado G, Dean J. Efficient estimation of word representations in vector space. arXiv. 2013:1301.3781v3. https://doi.org/10.48550/arXiv.1301.3781.

Moro V, Urgesi C, Pernigo S, Lanteri P, Pazzaglia M, Aglioti SM. The neural basis of body form and body action agnosia. *Neuron*. 2008:60(2):235–246. https://doi.org/10.1016/j.neuron.2008.09.022.

Noirhomme Q, Lesenfants D, Gomez F, Soddu A, Schrouff J, Garraux G, Luxen A, Phillips C, Laureys S. Biased binomial assessment of cross-validated estimation of classification accuracies illustrated in diagnosis predictions. *Neuroimage Clin*. 2014:4:687–694. https://doi.org/10.1016/j.nicl.2014.04.004.

Ogden JA. Autotopagnosia: occurrence in a patient without nominal aphasia and with an intact ability to point to parts of animals and objects. *Brain*. 1985:108(4):1009–1022. https://doi.org/10.1093/brain/108.4.1009.

Oldfield RC. The assessment and analysis of handedness: the Edinburgh inventory. *Neuropsychologia*. 1971:9(1):97–113. https://doi.org/10.1016/0028-3932(71)90067-4.

Oosterhof NN, Wiggett AJ, Diedrichsen J, Tipper SP, Downing PE. Surface-based information mapping reveals cross-modal vision–action representations in human parietal and

occipitotemporal cortex. *J Neurophysiol*. 2010:104(2):1077–1089. https://doi.org/10.1152/jn.00326.2010.

Orlov T, Makin TR, Zohary E. Topographic representation of the human body in the occipitotemporal cortex. *Neuron*. 2010:68(3): 586–600. https://doi.org/10.1016/j.neuron.2010.09.032.

Paillard J. Body schema and body image-a double dissociation. In: Gantchev GN, Mori S, Massion J, editors. *Motor control, today and tomorrow*. Academic Publishing House "Prof. M. Drinov", Sofia, Bulgaria, 1999:197–214.

Peirce J, Gray JR, Simpson S, MacAskill M, Höchenberger R, Sogo H, Kastman E, Lindeløv JK. Psychopy2: experiments in behavior made easy. *Behav Res Methods*. 2019:51(1):195–203. https://doi.org/10.3758/s13428-018-01193-y.

Pick A. Störung der orientierung am eigenen körper. *Psychol Forsch*. 1922:1(1):303–318. https://doi.org/10.1007/BF00410392.

Popham SF, Huth AG, Bilenko NY, Deniz F, Gao JS, Nunez-Elizalde AO, Gallant JL. Visual and linguistic semantic representations are aligned at the border of human visual cortex. *Nat Neurosci*. 2021:24(11):1628–1636. https://doi.org/10.1038/s41593-021-00921-6.

Řehůřek R, Sojka P. 2010. Software Framework for Topic Modelling with Large Corpora. *Proceedings of the LREC 2010 Workshop on New Challenges for NLP Frameworks*. https://doi.org/10.13140/2.1.2393.1847.

Rizzolatti G, Sinigaglia C. The functional role of the parieto-frontal mirror circuit: interpretations and misinterpretations. *Nat Rev Neurosci*. 2010:11(4):264–274. https://doi.org/10.1038/nrn2805.

Sacchett C, Humphreys GW. Calling a squirrel a squirrel but a canoe a wigwam: a category-specific deficit for artefactual objects and body parts. *Cogn Neuropsychol*. 1992:9(1):73–86. https://doi.org/10.1080/02643299208252053.

Schwoebel J, Coslett HB. Evidence for multiple, distinct representations of the human body. *J Cogn Neurosci*. 2005:17(4):543–553. https://doi.org/10.1162/0898929053467587.

Schwoebel J, Coslett HB, Buxbaum LJ. Compensatory coding of body part location in autotopagnosia: evidence for extrinsic egocentric coding. *Cogn Neuropsychol*. 2001:18(4):363–381. https://doi.org/10.1080/02643290126218.

Seabold S, Perktold J. Statsmodels: econometric and statistical modeling with python. In: van der Walt S, Millman J, editors. *Proceedings of the 9th Python in Science Conference*, 2010. p. 92–96. https://doi.org/10.25080/Majora-92bf1922-011.

Semenza C. Impairment in localization of body parts following brain damage. *Cortex*. 1988:24(3):443–449. https://doi.org/10.1016/S0010-9452(88)80007-8.

Shelton JR, Fouch E, Caramazza A. The selective sparing of body part knowledge: a case study. *Neurocase*. 1998:4(4–5):339–351. https://doi.org/10.1080/13554799808410631.

Simmons WK, Barsalou LW. The similarity-in-topography principle: reconciling theories of conceptual deficits. *Cogn Neuropsychol*. 2003:20(3–6):451–486. https://doi.org/10.1080/02643290342000032.

Sirigu A, Grafman J, Bressler K, Sunderland T. Multiple representations contribute to body knowledge processing. Evidence from a case of autotopagnosia. *Brain*. 1991:114(1):629–642. https://doi.org/10.1093/brain/114.1.629.

Spiridon M, Fischl B, Kanwisher N. Location and spatial profile of category-specific regions in human extrastriate cortex. *Hum Brain Mapp*. 2006:27(1):77–89. https://doi.org/10.1002/hbm.20169.

Suzuki K, Yamadori A, Fuji T. Category-specific comprehension deficit restricted to body parts. *Neurocase*. 1997:3(3):193–200. https://doi.org/10.1080/13554799708404054.

Tanaka K. Inferotemporal cortex and object vision. *Annu Rev Neurosci*. 1996:19(1):109–139. https://doi.org/10.1146/annurev.ne.19.030196.000545.

Tong J, Binder JR, Humphries C, Mazurchuk S, Conant LL, Fernandino L. A distributed network for multimodal experiential representation of concepts. *J Neurosci*. 2022:42(37):7121–7130. https://doi.org/10.1523/JNEUROSCI.1243-21.2022.

Urgesi C, Berlucchi G, Aglioti SM. Magnetic stimulation of extrastriate body area impairs visual processing of nonfacial body parts. *Curr Biol*. 2004:14(23):2130–2134. https://doi.org/10.1016/j.cub.2004.11.031.

Urgesi C, Candidi M, Ionta S, Aglioti SM. Representation of body identity and body actions in extrastriate body area and ventral premotor cortex. *Nat Neurosci*. 2007:10(1):30–31. https://doi.org/10.1038/nn1815.

Vignemont F. How many representations of the body? *Behav Brain Sci*. 2007:30(2):204–205. https://doi.org/10.1017/S0140525X07001434.

Vignemont F. Body schema and body image—pros and cons. *Neuropsychologia*. 2010:48(3):669–680. https://doi.org/10.1016/j.neuropsychologia.2009.09.022.

Warrington EK, McCarthy RA. Categories of knowledge: further fractionations and an attempted integration. *Brain*. 1987:110(5): 1273–1296. https://doi.org/10.1093/brain/110.5.1273.